IRAQI Academic Scientific Journals
Iraqi Journal of Civil Engineering
Available online at https://www.iasj.net/
Journal homepage: https://www.iasj.net/iasj?func=issues&jId=141&uiLanguage=en

# Impact of Ground Motion Selection on The Seismic Assessment of Reinforced Concrete Buildings

***Ammar Shanta Alshaheen*[*1], *Samir A.J. Aljassim*[2]**

[1]Department of Civil Engineering, University of Basrah, Basrah, Iraq, eng.a.alshaheen@gmail.com

[2]Department of Civil Engineering, University of Almaaqal, Basrah, , samiraljassim@gmail.com

ARTICLEINFO

*Article history:*
Received 17 /07 / 2021.
Received in revised form 10 /12/ 2021.
Accepted 11 /12 / 2021
Available online 28/02 / 2022

Keywords:
Ground motion selection;
Seismic assessment;
Nonlinear time history analysis;
ASCE7
Reinforced Concrete Buildings

ABSTRACT

The goal of this study is to determine the impact of ground motion recordings (GMs) selection on the seismic performance evaluation of reinforced concrete (RC) structures. From three GMs in ASCE7-10 to eleven GMs in ASCE7-16, the ASCE7 has upgraded the minimum GMs utilized in seismic analysis, When the GMs are used to evaluate an existing structure, the earthquake load may under or overestimate the structure's capacity. The case study is an existing RC building, dual system, and unsymmetric in-plane and height. Because of these asymmetries, the Non-linear Time History Analysis (NTHA) is the most accurate method. It is performed for 30 GMs in directions X and Y. The GMs were chosen and scaled to meet the Basrah city response spectrum curve (RSC), which is based on the existing Iraqi seismic code. The study parameters that were investigated are included story implication ratio, torsional irregularity index, floor rotation angle, and plastic hinge formation. These parameters are investigated in three cases. The selection of GMs for Case 1 and 2 are based on the ASCE7-10 while Case 3 is based on ASCE7-16. The comparison between cases is shown a considerable difference in structural response could lead to various retrofitting decisions. The findings revealed that existing RC buildings constructed in accordance with ASCE7-10, particularly medium and high-rise structures, should be re-evaluated.

DOI: **10.37650/ijce.2021.172874**

## 1. Introduction

Earthquakes expose many flaws in building design and inadequate performance to resist seismic loads. These flaws are being investigated by scientific research and subsequently updated seismic limitations in codes to prevent future building collapse by enhancement their performance. It is unreasonable to ignore the existence of structures built to older codes. Often, there are no legislations accessible to reassess structures seismic performance to the updated codes, while it may be considered more dangerous than those built with updated code versions. Because they are probably built with minimum seismic limits and do not achieve acceptable seismic performance according to modern codes. Also, they are probably classified as collapsible to updated codes at increasing building safety in earthquakes. For example, the American standers, ASCE7-10 ((ASCE/SEI 7-10) 2010), are accepted three GMs as a minimum for earthquake analysis/design. Similarly, in the updated version ASCE7-16 ((ASCE/SEI 7-16) 2017), the minimum GMs are increased to seven, causing concern about the impact of this increase on the analysis/design outcomes. The method of selecting suitable seismic GMs is

*Correspondence: eng.a.alshaheen@gmail.com

another important factor that influences the output of the seismic performance evaluation of buildings, which is a challenge in and of itself to obtain adequate findings. The engineering community uses several methods to selecting GMs, such as the Mean Condominium method and the Peer online tool. The GMs must also be scaled to be compatible with the target area and to replicate the character of the ground and the significance of the buildings. Another important consideration is selecting an analysis method among the several that are commonly used in the engineering community, such as Pushover and Nonlinear Time History Analysis (NTHA). Pushover despite their results are underestimated the expected seismic effect (Hussain and Aljassim 2021), while NTHA is considered to be more accurate, it is excluded because its output is difficult to control and is related to the GMs data used (Eelangga, Teguh, and Makrup 2020). The important part of getting reliable results from the NTHA method is to select GMs that accurately predict a future earthquake(Morris et al. 2019). The requirements for GMs selection are relatively open to interpretation, while it can result in significant differences in structural response, which could lead to different retrofitting decisions. So that, the number of GMs required in the codes should be increased (Uribe et al. 2019). This study investigates the impact of the number of GMs on seismic analysis and outputs using a case study of an RC building built in Basrah, southern Iraq. The Iraqi seismic code 1997 (Control 1997) categorized southern Iraq as a moderate impact area, but the current code 2017 (Iraq 2017) has been modified based on seismic activity in Iraq in general and studies that predicts an increase in seismic activity. The building is seismically assessed using NTHA under two versions of the American standers ASCE7 -10 and ASCE 7-16, for a different number of GMs. The seismic requirements of the codes still need to be enhanced, particularly in terms of taking into consideration the influence of extensive vertical GM generated by near-source earthquakes (Hosseini, Hashemi, and Safi 2017).

## 2. Building Description and Modeling

The case study is RC dual system building with shear walls, which is designed in 2011 to be a private hospital, and then the design was modified to a five stars hotel. The architecture design of the building includes asymmetric in-plane and height as shown in Fig.1a. The three-dimensional building is modeled in SAP2000 software ( Computers & Structures, Inc.) as shown in Fig.1b. The plan of building ground floor is illustrated in Fig.1c, and the three corners of the building are used as control points in the calculation of the results; they are labeled as Cr1, Cr2, and Cr3. Due to these asymmetric, the NTHA is the most accurate method to be used (Patil and Kumbhar 2013). The total height of the building is 48m. The first-floor height is 5.5m, the third, fifth, and eighth storeys are 5m while the other floor heights are 4m. The beams and columns are modeled as frame elements, the slabs are modeled as shell elements, the shear walls are modeled as multi-layered shell elements and the building is assumed fixed at the foundation level. The partitions are not considered in the analysis. At the beginning and end of each beam (5% and 95% of the length) plastic hinges of the type (moment M3 and shear V2) are assigned. In the columns, plastic hinges of the type P-M1-M2 (combined axial with a moment in two directions) and torsion (T) are assigned at (5% and 95% of the length). Slabs are assumed linear materials, which operate as a rigid diaphragm in each floor level to transfer lateral forces caused by seismic loads to the columns. Finally, shear wall nonlinearity is presented as a multi-layer shell element model (MLSE) based on composite material mechanics principles (Jarallah and Taki 2017). It is composed of a number of layers with varying thicknesses and material properties, including reinforcing rebars smeared into one or more layers. Furthermore, there is no relative displacement between the steel and concrete layers, and the material properties of each layer remain constant across the layer thickness (Lu and Guan 2021). The material properties modeled in the SAP2000 program are given in Table1, the Mander model (Mander, Priestley, and Park 1988) for concrete and Chai's model for steel are used (Chai, Priestley, and Seible 1991)

**Table 1. Properties of Material**

| SN | Property | Amount |
|---|---|---|
| Concrete | Compression strength, cylinder (Mpa) | 35 |
| | Poisson ratio | 0.2 |
| | Concrete unit weight ($\rho_c$) (kN/m$^3$) | 24 |
| | Concrete modulus of elasticity ($E_c$)* (Mpa) | 27.8056x10$^3$ |
| Steel | Yield Stress (Mpa) | 420 |
| | Poisson ratio | 0.3 |

| | |
|---|---|
| Steel modulus of elasticity ($E_c$) (Mpa) | $2x10^5$ |

* For normal weight concrete. ASCI 318-19 , 19.2.2.1.((ACI) 2019)

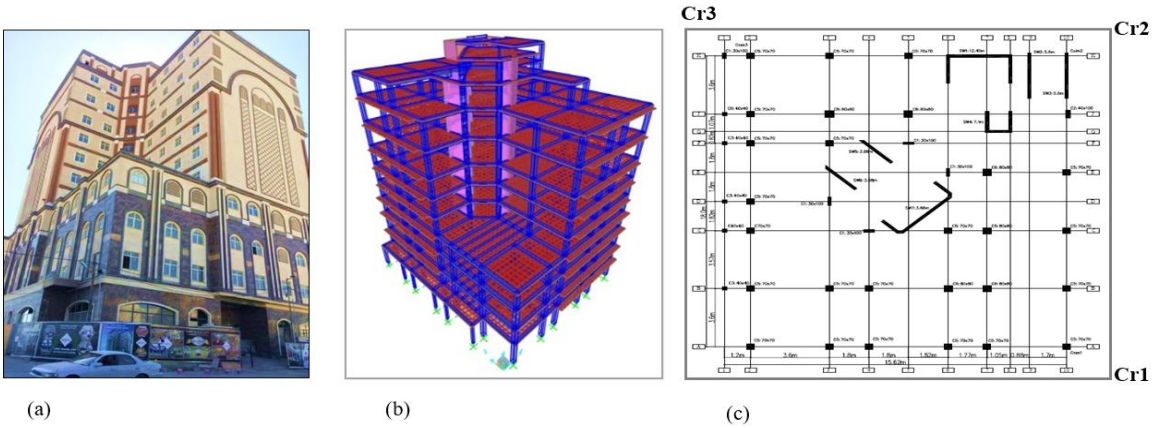


**Figure1. (a) the perspective view of the building (b) the 3D model, (c) the plan of the ground floor**

## 3. GMs and Response Spectrum Curve (RSC)

To perform the analysis, real 30 GMs are selected by using the PEER online tool based on the RSC of Basrah city. The GMs are available in PEER online databases (PEER NGA-West2), and are applied in the horizontal direction; the GMs used are not inserted to brief. The GMs have different magnitudes and intensities, to be applied for Basrah city, so they should be scaled to their level of earthquakes. The spectrum matchings method is used to scale the selected GMs. The RSC of Basrah is done based on the Iraqi seismic code in 2017 (ISC 2017) (Iraq 2017) as shown in Fig.2a. Each of the thirty GMs is scaled using SeismoMatch 2021 software. The GMs are applied either in X-direction or Y-direction. The geometric nonlinearity is conducted in analysis by using the P-delta method.

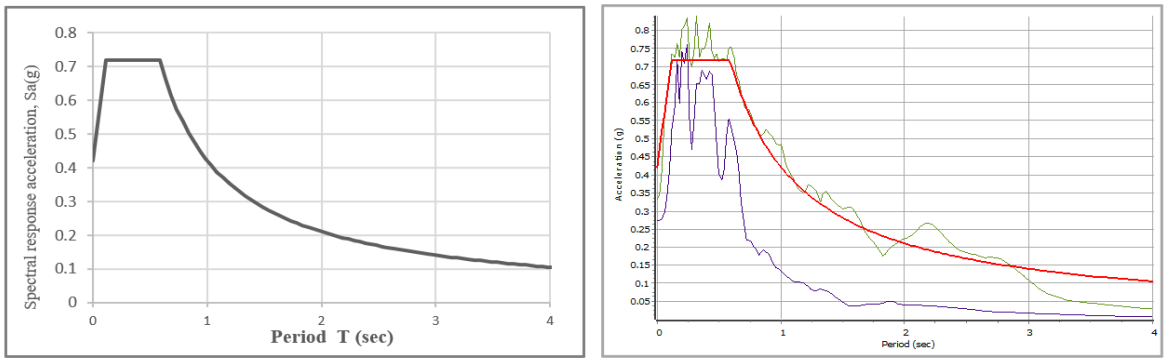


**Figure2. (a) RSC of Basrah city based on ISC2017 (Iraq 2017), (b) GM4 matching with Basrah RSC**

## 4. Torsion in Buildings

Buildings are built in a variety of shapes for comfort and efficiency, which is leads to asymmetric structural systems. Asymmetric is the major cause of torsion under earthquake loads. The earthquake load applies at the structure's center of mass (CM) and resistive force operates at the center of rigidity (CR). Torsional problems occur when the CM and the CR are not in the same position. By increasing, the distance between them the structure (Eccentricity) is pushed to rotate around the rigid structural section (rigid core) and is subjected to large torsional moments (Gokdemir et al. 2013), as shown in Fig.3. (Mahdi Yazdinezhad 2016). Torsion effects

are unavoidable, which is the weakest point in a building (Sesigiir et al. 2001). Most seismic codes provide recommendations for reducing the effects of torsion by an increase in strength for elements on the weak side of the building or a decrease in strength on the strong side. It is also important to note that isolating large building sections from each other reduces torsion effects (Gokdemir et al. 2013). Shear wall elements should also be placed outside the building (İlgün and Yorulmaz 2021). In this study, the torsional behavior is studied using two parameters:

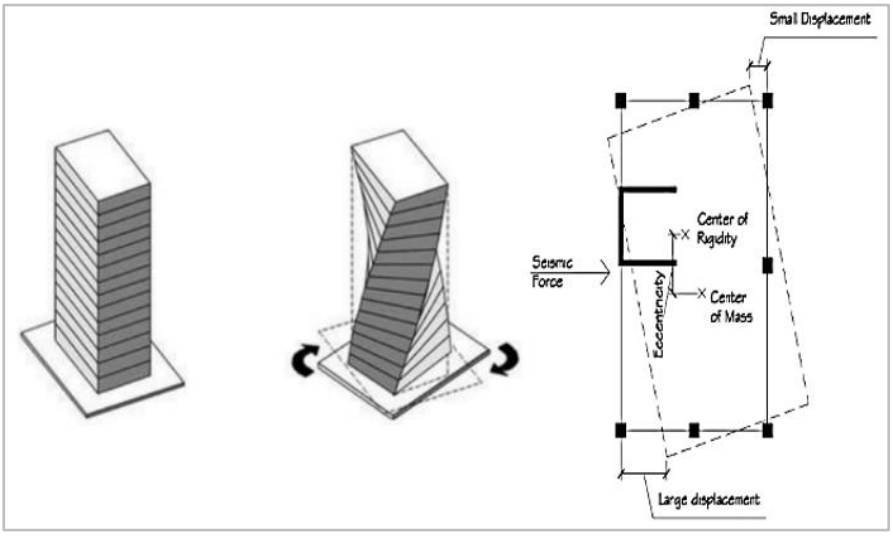


**Figure3. Definitions of CM, CR, and Eccentricity [26]**

## *4.1. Torsional Irregularity Ratio (TIR)*

TIR is used to determine existing torsional behavior but does not accurately reflect torsional behavior (Yavuz 2014). It is defined by ASCE7 to assess whether or not a horizontal irregularity exists (DeBock et al. 2013). Horizontal irregularity exists when the TIR is greater than 1.2, and extreme torsional irregularity exists when it is greater than 1.4 ASCE7-16 ((ASCE/SEI 7-16) 2017). The term "extreme torsional irregularity" was not specified in previous codes, but due to the importance of the issue, the topic is now clarified in considerable detail (Aliakbari, Garivani, and Shahmari 2020). TIR evaluation, as shown in Equ.1 and Fig.4a.

$$TIR = \delta_{max}/\delta_{ave} \quad (1)$$

Where; $\delta_{max}$= the maximum displacement at level x, and $\delta_{ave}$= the average of the displacements at the extreme points of the structure at level x.

## *4.2. Floor Rotation Angle (FRA)*

The FRA (Θ) closely reflects the torsional behavior of buildings and is considered to be a direct representation of torsional compatibility with the TIR (Yavuz 2014). It is an important parameter for evaluating torsion moment plus the possibility of local failure for an outer element, threatening the stability of a structure that is highly dependent on the diaphragms' performance (Ahmed et al. 2016). Equ.2 is used to calculate FRA, as shown in Fig.4b.

$$\theta = (\delta_A - \delta_B)/L \quad \text{(radian)} \quad (2)$$

Where; $\delta_A$ =Displacement at control node A at level x, $\delta_B$ =Displacement at control node B at level x, and L=the distance between A and B at level x.

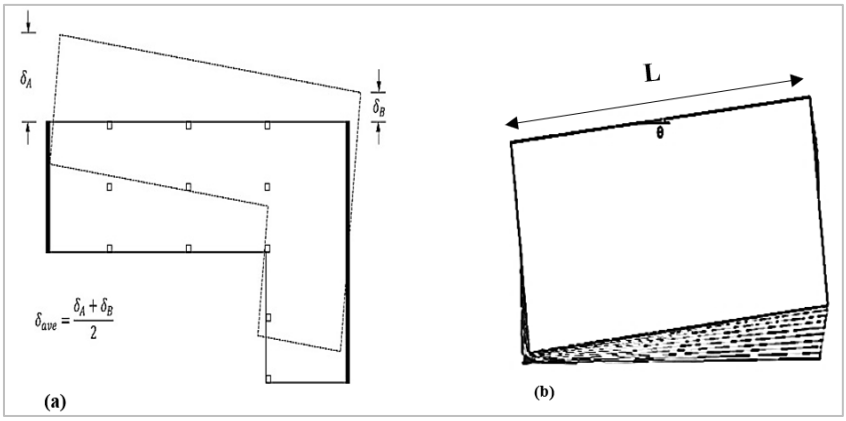


**Figure4. Definition of (a) TIR (ASCE7-16), (b) FRA (Ɵ ) (Yavuz 2014)**

### *4.3. Story Drift Ratio (SDR)*

The Drift "shall be computed as the largest difference of the deflections of vertically aligned points at the top and bottom of the story under consideration along any of the edges of the structure" ((ASCE/SEI 7-16) 2017). The floors were modeled as rigid diaphragms, and the displacement was taken into account as deflection. The displacement of nodes at Cr1 is showed the highest values compared with Cr2 and Cr3, due to the influence of the position of shear walls. The displacements were taken as absolute values. SDR is the floor drift divided at its height, As shown in Equ.3. The SDR can affect structural elements, nonstructural elements, and surrounding structures, and the effect increases in proportion to the irregularity of the building (Ahmed et al. 2016).

$$SDR = \Delta_i / h_i \quad (3)$$

Where; $\Delta_i$= story drift, it is the difference between two successive stories displacement at the same time, and $h_i$ = story height.

For general structures and risk category, I or II the allowable drift ($\Delta_i$) is 0.02 $h_i$. "The mean story drift ratio shall not exceed two times the limits of Table 12.12-1" ((ASCE/SEI 7-16) 2017). It is concluded, the allowed SDR is ($4x10^{-2}$). In the updated code allowable drift limit increased by 60 %.

## 5. Cases Studied

The results of the analysis are given as; displacement of selected nodes (at control points), SDR, FRA, TIR, and plastic hinges formation. It is sorted upward and calculates the total average (Av) to be a reference. The three cases below are used to compare the variations of the response for a different number of GMs. Case1; Select three GMs based on ASCE7-10. To compare the effects on the results between selecting the first three GMs (F3) and the last three GMs (L3) (maximum results of three), calculate the differences (DFs) between F3 and L3 (F3&L3), F3 and Av (F3&Av), and L3 and Av (L3&Av). Case2; select seven GMs based on ASCE7-10. Compare the effects on the results between selecting the first seven GMs (F7) and the last seven GMs (L7) (average results of three). Calculate the DFs between F7 and L7 (F7&L7), F7 and Av (F7&Av), and L7 and Av (L7&Av). Finally, Case3, select fifteen GMs based on ASCE7-16. A comparison of the effects on the results between selecting the first seven GMs (F15) and the last seven GMs (L15) (average results of three) is presented in this case. Calculate DFs between F15 and L15 (F15&L15), F15 and Av (F15&Av), and L15 and Av (L15&Av). To compare between cases, calculate the differences between cases, first between cases (2) and (1) to illustrate the contrast in building response in the same code, ASCE7-10, then between Cases (3) and (1) and Cases (3) and (2) to illustrate the contrast between two codes ASCE7-16 and ASCE7-10.

# 6. Results and Discussion

## *6.1. Displacement of control nodes*

As shown in Figures (5a) and (6a), the maximum displacements in all cases are in the X-direction. It is an indicator that the building stiffness is greater in the Y-direction than in the X-direction. As shown in Table 2 and Figures (5) and (6), Case3 has the lowest (F&L) DFs and Case1 has the highest DFs when compared to the other cases. Observe the curves in the Figures, noting that Case3 is the closest to the Av. The comparison between case3 and cases 1 and 2 is shown a substantial variance between the findings, indicating that the increasing number of GMs is crucial for the accuracy of the results, as shown in Fig.7. The comparison of case2 with the case shows that selecting 7 GMs is more accurate than selecting three based on the same code.

**Table 2. Maximum displacements and the VRs in directions X and Y, cases 1-3**

| | F, cm | L, cm | (F3&L3) | (F3&Av) | (L3&Av) |
|---|---|---|---|---|---|
| Cases | | | X-direction | | |
| 1 | 11 | 22.5 | 11.5 | 6.1 | 5.4 |
| 2 | 12.7 | 20.7 | 8 | 4.4 | 3.6 |
| 3 | 15 | 19.2 | 4.2 | 2.1 | 2.1 |
| Cases | | | Y-direction | | |
| 1 | 12.6 | 17.8 | 5.2 | 1.3 | 4.2 |
| 2 | 10.3 | 15.7 | 5.4 | 3.3 | 2.1 |
| 3 | 12.1 | 15.1 | 3 | 1.5 | 1.5 |

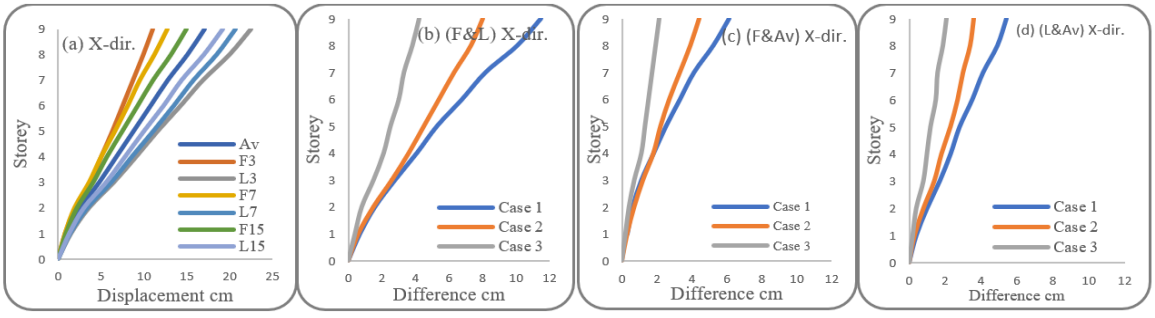


**Figure.5. Displacements and DFs of Cases 1-3 in the X-direction (a) displacements (b) (F&L) (C) (F&Av) (d) (L&Av)**

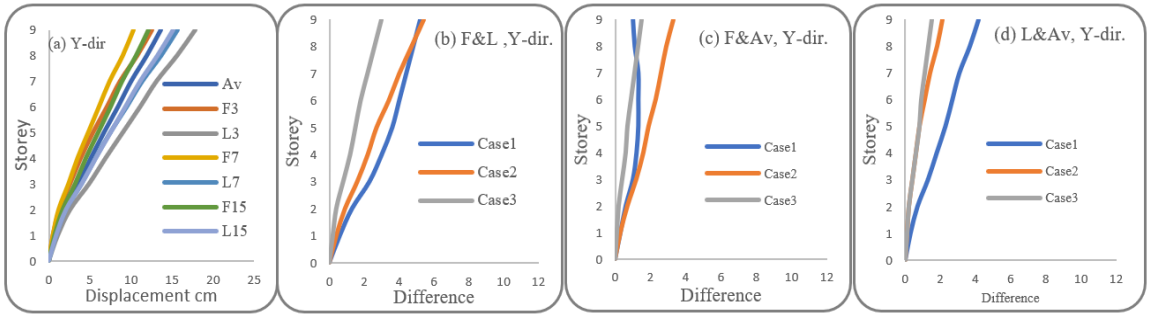


**Figure.6. Displacements and DFs of Cases 1-3 in the Y-direction (a) displacements (b) (F&L) (C) (F&Av) (d) (L&Av)**

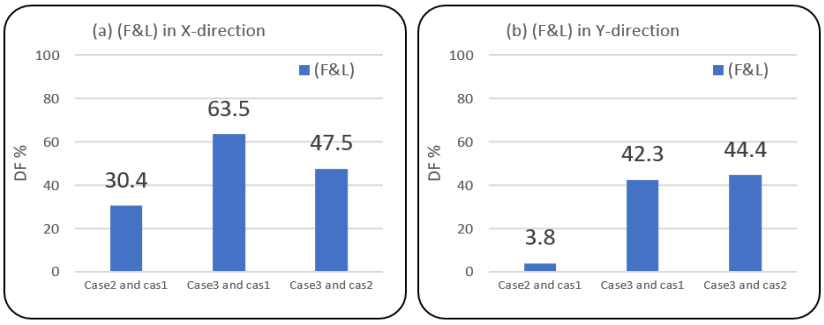


**Figure7. The absolute values of DFs % of maximum displacement for (F&L) to cases 1-3 in (a)X- direction, (b) Y-direction**.

## *6.2. Story Drift Ratio (SDR)*

As shown in Table 3 and Figures (8a) and (9a), the SDR results are much lower than the ASCE7-16 code allowed limits in all cases, and the values in the X-direction are higher than the values in the Y-direction. This explains the building has a high stiffness for lateral displacement, and the stiffness is higher in the Y-direction than in the X-direction. Also, based on SDRs, the middle level is more vulnerable to seismic load than the upper and lower floors. As shown in Table 3 and Figures (8) and (9), case 3 analysis with 15 GMs has the lowest DFs in the results, while case 1 analysis with 3 GMs has the highest DFs . Furthermore, case 3 is the closest to the Av when compared to cases 1 and 2, which show a significant gap in the results. Similarly to displacement results, comparing cases 1, 2, and 3 shows that case 3 analysis with 15 GMs is much better accuracy than other cases. which concluded that increasing the number of GMs is essential in reducing the gap in the findings, highlighting the need of updating the seismic code. Also, using seven GMs provides better results than using three (comparing case 2 to case 1). The cases DFs comparisons are shown in Fig.10.

**Table 3 Maximum SDR and the DFs % in directions X and Y, cases 1-3**

| | F ($x10^{-2}$) | L ($x10^{-2}$) | (F3&L3) | (F3&Av) | (L3&Av) |
|---|---|---|---|---|---|
| Cases | | | X-direction | | |
| 1 | 0.34 | 0.68 | 0.38 | 0.21 | 0.17 |
| 2 | 0.38 | 0.61 | 0.23 | 0.13 | 0.1 |
| 3 | 0.45 | 0.57 | 0.12 | 0.06 | 0.06 |
| Cases | | | Y-direction | | |
| 1 | 0.39 | 0.52 | 0.17 | 0.05 | 0.12 |
| 2 | 0.32 | 0.48 | 0.18 | 0.1 | 0.08 |
| 3 | 0.37 | 0.46 | 0.09 | 0.05 | 0.05 |

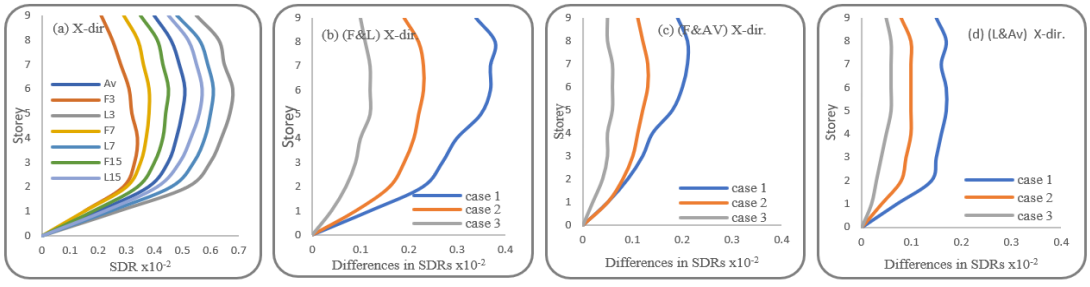


**Figure 8. SDRs and DFs of Cases 1-3 in the X-direction (a) SDRs (b) (F&L) (C) (F&Av) (d) (L&Av) (L&Av)**

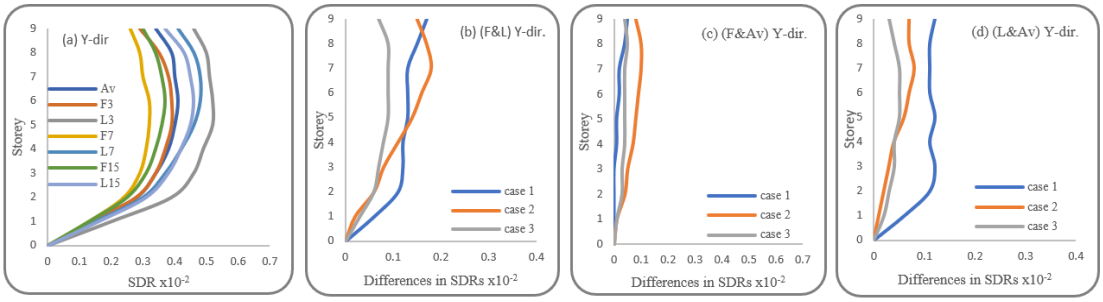


Fig.9. SDRs and DFs of Cases 1-3 in the Y-direction (a) SDRs (b) (F&L) (C) (F&Av) (d) (L&Av)

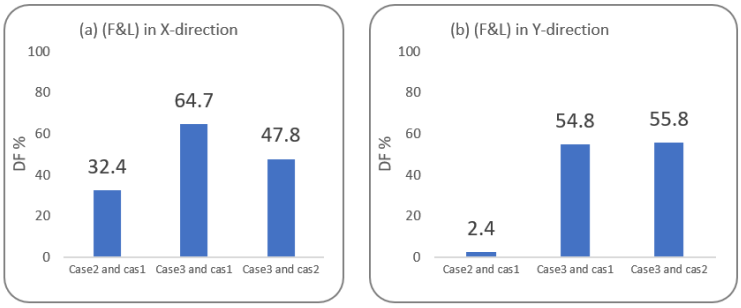


**Figure 10. The absolute values of DFs % of maximum SDR for (F&L) to cases 1-3 in (a)X- direction, (b) Y-direction**

## *6.3. Floor Rotation Angle (FRA)*

As shown in Table 4 and Figures(11) and (12), FRAs in the X-direction are higher than in the Y-direction, which reflected the building's torsional stiffness is higher in the X-direction. Case 3 shown minimum DFs compared with other cases and it is the closest to the average. As shown in Fig.13, the comparing between cases is shown that case 3 has lower DFs, and case1 is the greatest. That indicator that increasing of GMs enhancement the findings.

**Table 4 Maximum FRAs and PDRs in directions X and Y, cases 1-3**

| | F (x10$^{-5}$ radian) | L (x10$^{-5}$ radian) | (F3&L3) | (F3&Av) | (L3&Av) |
|---|---|---|---|---|---|
| Cases | | X-direction | | | |
| 1 | 3.96 | 7.03 | 3.07 | 1.47 | 1.62 |
| 2 | 3.3 | 6.69 | 3.39 | 2.11 | 1.28 |
| 3 | 4.43 | 6.39 | 1.96 | 0.98 | 0.98 |
| Cases | | Y-direction | | | |
| 1 | 5.42 | 7.4 | 1.98 | 0.67 | 1.31 |
| 2 | 4.59 | 7.05 | 2.46 | 1.5 | 0.96 |
| 3 | 5.4 | 6.79 | 1.39 | 0.69 | 0.7 |

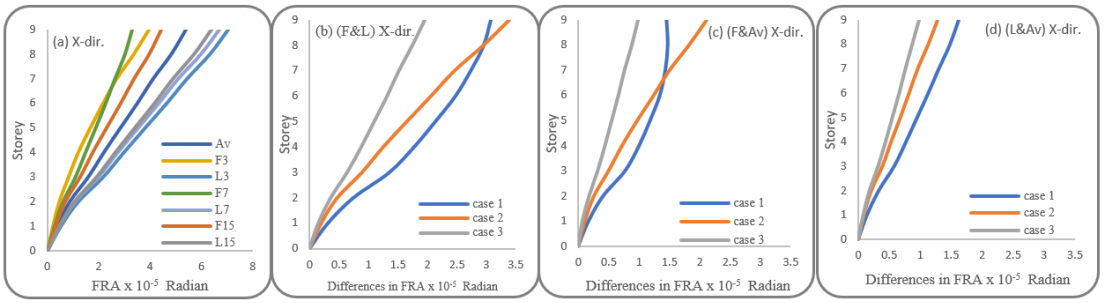


**Figure11. FRAs and DFs of Cases 1-3, in the X-direction (a) FRAs (b) F&L (C) F&Av (d) L&Av**

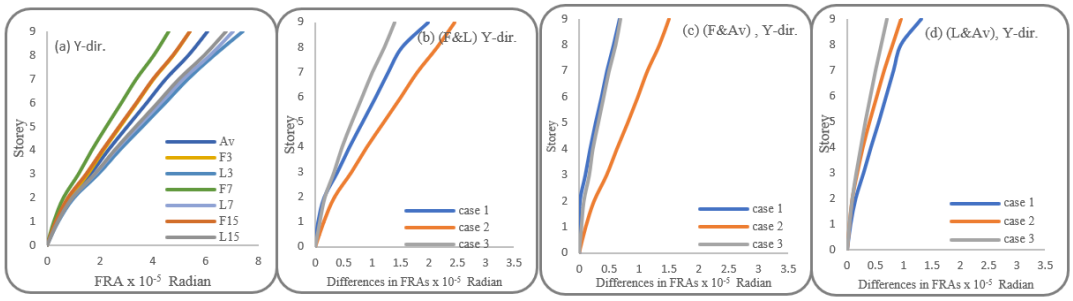


**Figure12. FRAs and DRs of Cases 1-3 in, the Y-direction (a) FRAs (b) F&L (C) F&Av (d) L&Av**

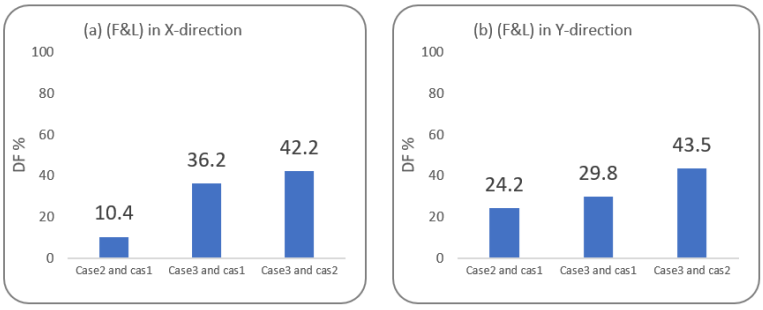


**Figure13. The absolute values of DFs % of maximum FRAs for (F&L) to cases 1-3 in (a)X- direction, (b) Y-direction.**

## *6.4. Torsional Irregularity Ratio (TIR)*

As shown in Table 5, the maximum value of TIRs for (F) for cases (1) and (2), are 1.33 and 1.37 respictively, which mean the torsional irregularity is exist, while for (L) is 1.92 and 1.76 which mean the extreme torsional irregularity. In these cases the designated type of torsion differs depending on the GMs used. Case 3 shows TIRs more than 1.4 for each (L) and (F), indicating that the Building torsion is extreme. As shown in Figures (14) and (15), the TIRs in the X-direction are smaller than those in the Y-direction, which reflect structure torsional stiffness in X-direction is higher in the Y-direction. Case 3 is closest to AV, and it has lower DFs comparing with cases 1 and 2 as shown in Fig.16 . TIR is provided another indicator that the number of selection GMs has a considerable effect on the results.

**Table 5 Maximum TIRs and DFs in directions X and Y, cases 1-3**

| | F | L | (F3&L3) | (F3&Av) | (L3&Av) |
|---|---|---|---|---|---|
| Cases | | | X-direction | | |
| 1 | 1.33 | 1.92 | 0.61 | 0.24 | 0.38 |
| 2 | 1.37 | 1.76 | 0.39 | 0.2 | 0.2 |
| 3 | 1.45 | 1.7 | 0.26 | 0.13 | 0.13 |
| Cases | | | Y-direction | | |
| 1 | 1.87 | 2 | 0.23 | 0.08 | 0.15 |
| 2 | 1.82 | 1.98 | 0.27 | 0.17 | 0.13 |
| 3 | 1.89 | 1.94 | 0.14 | 0.07 | 0.07 |

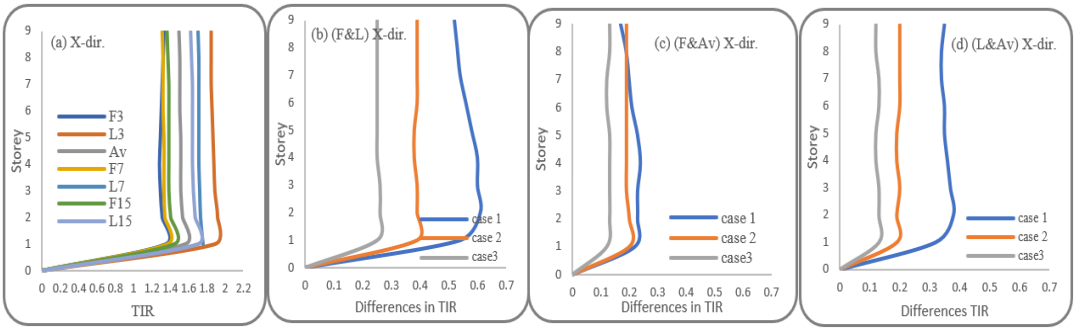


**Figure14. TIRs and DFs of Cases 1-3 in the X-direction (a) TIRs (b) F&L (c) F&Av (d)L&Av**

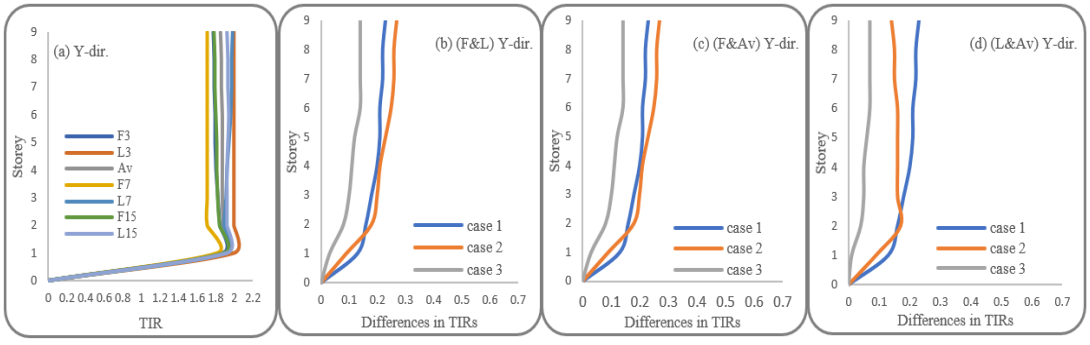


**Figure15. TIRs and DFs of Cases 1-3 in the Y-direction (a) TIRs (b) F&L (C) F&Av (d)L&Av**

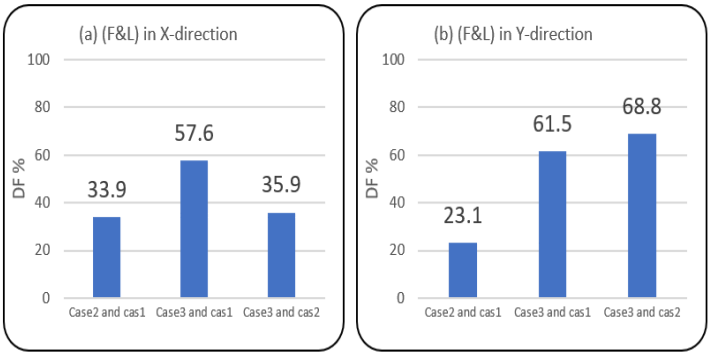


**Figure16. The absolute values of DFs % of maximum TIRs for (F&L) to cases 1-3 in (a)X- direction, (b) Y-direction.**

### *6.5. Plastic hinges*

The plastic hinge state (IO-LS) is only formed in beam elements of type M3, which explain the building behaviour under the weak beam strong column rule. The number of plastic hinges in the X-direction is more than in the Y-direction, as shown Fig.17, which explains the building has a higher stiffness Y-direction. As shown in Fig.17, case 3 has minimum DFs. The comparing between cases is shown that case 3 analysis with 15 GMs has lower DFs, and case1 is the greatest. It is concluded, increasing of GMs enhancement the findings. It is founded the plastic hinges formed especially at the coupling beams that connect two shear walls. Coupling beams have a small span-to-depth ratio, and their inelastic behaviour is typically influenced by the high shear pressures that occur in these components. It is usually stiffer and stronger than if they functioned separately ((FEMA273) 1997).

**Table 6 Maximum plastic hinge of type M3 and PDRs in directions X and Y, cases 1-3**

| | F (Number) | L (Number) | (F3&L3) | (F3&Av) | (L3&Av) |
|---|---|---|---|---|---|
| Cases | | | X-direction | | |
| 1 | 15 | 39 | 24 | 9 | 15 |
| 2 | 16 | 32 | 16 | 8 | 8 |
| 3 | 19 | 28 | 9 | 5 | 4 |
| Cases | | | Y-direction | | |
| 1 | 1 | 8 | 7 | 1.97 | 5.03 |
| 2 | 0.71 | 6.14 | 5.43 | 2.26 | 3.17 |
| 3 | 1.89 | 1.94 | 3.13 | 1.57 | 1.56 |

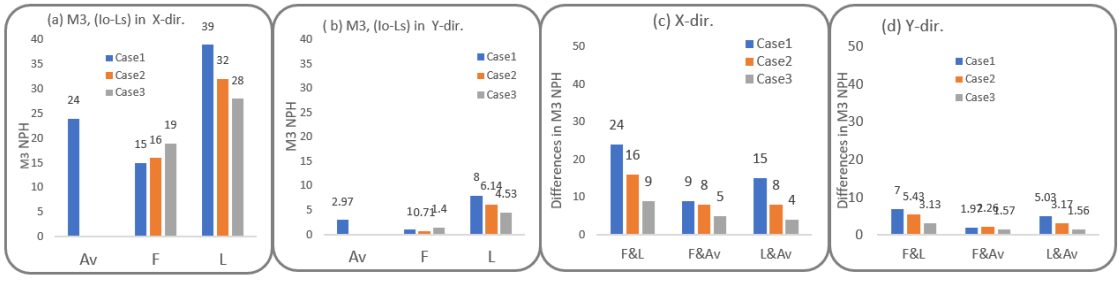


**Figure.17. The plastic hinge number of types M3, state (IO-LS) for cases 1 to 3 in (a) X-direction, (b) Y-direction, and DFs in (c) X- direction, (d) Y-direction.**

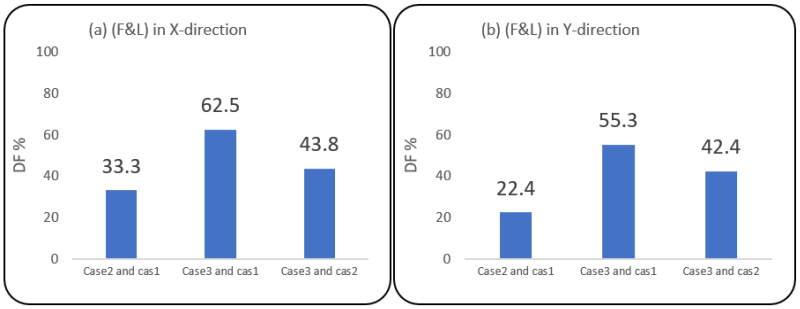


**Figure18. The absolute values of maximum DFs (F&L) of M3 plastic hinge number for the cases 1-3 in (a)X- direction, (b) Y-**

## 7. Conclusions

The following are the study's conclusions, based on the findings:

1. Updating the selection number of GMs in ASCE7-16 was necessary because increasing the number of GMs employed in the analysis contributes to accuracy and reduces differences.
2. Based on the ASCE7-10 code, selecting seven GMs for seismic assessment produced significantly better results than selecting three.
3. The seismic assessment of the RC building showed acceptable performance, but retrofitting is necessary especially for the coupling beams that connect shear walls to decrease the number and level of plastic hinges formed during earthquakes.

## References

(ACI), American Concrete Instirute. 2019. "Building Code Requirements for Structural Concrete (ACI 318-19) Commentary on Building Code Requirements for Structural Concrete (ACI 318R-19)." October: 261.

(ASCE/SEI 7-10), American Society of Civil Engineers. 2010. *Minimum Design Loads for Buildings and Other Structures*.

(ASCE/SEI 7-16), American Society of Civil Engineers. 2017. American Society of Civil Engineers *Minimum Design Loads and Associated Criteria for Buildings and Other Structures*.

(FEMA273), Federal Emergency Management Agency. 1997. "NEHRP Guidelines for the Seismic Rehabilitation of Buildings." (October).

Ahmed, Momen M M, Shehata E Abdel Raheem, Mohamed M Ahmed, and Aly G A Abdel-shafy. 2016. "Irregularity Effects on the Seismic Performance of L-Shaped Multi Story Buildings." *Journal of Engineering Sciences Assiut University Faculty of Engineering* 44(September 2016): 513–36.

Aliakbari, Fatemeh, Sadegh Garivani, and Ali Shahmari. 2020. "Determination of Torsional Irregularity in Response Spectrum Analysis of Building Structures." *Structural Engineering and Mechanics* 5: 699–709.

Chai, Yuk Hon, M.J. Nigel Priestley, and Frieder Seible. 1991. October COLRET - A Computer Program for Strength and Ductility Calculation *Flexural Retrofit of Circular Reinforced Bridge Columns by Steel Jacketing*. Department ofApplied Mechanics and Engineering Sciences University of California.

Control, Ministry of industrial and mineral-centeral organaziation for standarazation and. 1997. *Iraqi Seismic Code Requirments for Buildings (Code 2/2017)*.

DeBock, D. Jared et al. 2013. "Importance of Seismic Design Accidental Torsion Requirements for Building Collapse Capacity." *International Association for Earthquake Engineering*.

Eelangga, Wisnu, Mochamad Teguh, and Lalu Makrup. 2020. "The Analysis of Performance Level on an Existing Multi-Story Building Structure Using the Time History Based on the Subduction Earthquake Source." In *E3S Web of Conferences*,.

Gokdemir, H. et al. 2013. "Effects of Torsional Irregularity to Structures during Earthquakes." *Engineering Failure Analysis* 35: 713–17. http://dx.doi.org/10.1016/j.engfailanal.2013.06.028.

Hosseini, Mahmood, Banafshehalsadat Hashemi, and Zahra Safi. 2017. "Seismic Design Evaluation of Reinforced Concrete Buildings for Near-Source Earthquakes by Using Nonlinear Time History Analyses." *Procedia Engineering* 199: 176–81.

Hussain, Shifaa N. A., and Samir A.J. Aljassim. 2021. "Seismic Evaluation of G+10 Stories Reinforced Concrete Shear Wall Building in South of Iraq." *Journal of Green Engineering (JGE)* 11(1).

İlgün, Abdülkerim, and Ahmet Mesut Yorulmaz. 2021. "Research on A1 Irregularity Status in Different Spectral Acceleration Coefficients on Reinforced Concrete Structures." *Turkish Journal of Engineering* 5(4): 177–82.

Iraq, Minist. Hous. Constr. 2017. *"Iraqi Seismic Code Requirements for Buildings 2017."* https://www.google.com/url?sa=i&url=https%3A%2F%2Famanatbaghdad.gov.iq%2Famanarules%2Fpict%2F%25D9%2585%25D8%25AF%25D9%2588%25D9%2586%25D8%25A7%25D8%25AA%2F%25D9%2585%25D8%25AF%25D9%2588%25D9%2586%25D8%25A9%2520%25D8%25A7%25D9%2584%25D8%25B2%25D9%2584%25D.

Jarallah, Husain Khalaf, and Zahir Noori M. Taki. 2017. "A Comparative Study on the Design Spectra Defined by Several Codes of Practice on RC Building Located in Baghdad City." In *Proceedings of the 4th Eng.*

*Conf. (21April 2016, Al-Nahrain Univ., Baghdad, IRAQ)*, Al-Nahrain Journal for Engineering Sciences (NJES), 425–35.

Lu, Xinzheng, and Hong Guan. 2021. Earthquake Disaster Simulation of Civil Infrastructures *Earthquake Disaster Simulation of Civil Infrastructures*.

Mahdi Yazdinezhad. 2016. *"Mitigating Torsional Irregularity Using Cross Laminated Timber-Reinforced Concrete Hybrid System,."* University of British Columbia. https://open.library.ubc.ca/collections/ubctheses/24/items/1.0228102 .

Mander, J B, M J N Priestley, and R Park. 1988. "Theoretical Stress-Strain Model for Confined Concrete." *Journal of Structural Engineering* 114(8): 1804–26.

Morris, Gareth J., Andrew J. Thompson, James N. Dismuke, and Brendon A. Bradley. 2019. "Ground Motion Input for Nonlinear Response History Analysis: Practical Limitations of NZS 1170.5 and Comparison to US Standards." *Bulletin of the New Zealand Society for Earthquake Engineering* 52(3): 119–33.

Patil, A S, and P D Kumbhar. 2013. "Time History Analysis of Multistoried Rcc Buildings for Different Seismic Intensities." *International journal of structural and civil engineering research* 2(August): 195–201.

PEER NGA-West2, Pacific Earthquake Engineering Research ( https://ngawest2.berkeley.edu )

Sesigiir, H, O C Celik, F Cili, and K Ozgen. 2001. "Effect of Structural Irregularities and Short Columns on the Seismic Response of Buildings during the Last Turkey Earthquakes." *Transactions of the Built Evironment* 57.

Uribe, Raul, Siamak Sattar, Matthew S. Speicher, and Luis Ibarra. 2019. "Effect of Common U.S. Ground Motion Selection Methods on the Structural Response of Steel Moment Frame Buildings." *Earthquake Spectra* 35(4): 1611–35. https://doi.org/10.1193/122917EQS268M.

Yavuz, Girgin. 2014. "Torsional Irregularity in Multi-Story Structures." : 121–31.